

Ultra-high energy neutrinos at the Pierre Auger Observatory

Inés Valiño*

Depto. Física de Partículas & Instituto Galego de Física de Altas Enerxías, Universidade de Santiago de Compostela, Spain

E-mail: inesvr@gmail.com

for the Pierre Auger Collaboration

Observatorio Pierre Auger, Av. San Martín Norte 304, 5613 Malargüe, Argentina

Full author list: http://www.auger.org/archive/authors_2017_03.html

The Pierre Auger Observatory is the largest ultra-high energy cosmic-ray detector built so far in the world. With the Surface Detector array of the Observatory we can also detect ultra-high energy neutrinos with energies around 100 PeV and above. The identification is efficiently done for neutrinos of all flavours interacting in the atmosphere at large zenith angles, as well as for tau neutrinos interacting in the Earth's crust, covering sky directions with equatorial declinations from about -80° to $+60^\circ$. The sensitivity obtained summing up all these channels is shown to be comparable to other neutrino detectors in operation, and to constrain several models of cosmic ray and neutrino production in the EeV region. In the absence of candidates in data from 1 January 2004 to 31 March 2017, improved stringent limits to diffuse and point source fluxes of ultra-high energy neutrinos are obtained. In addition, we report on the results of the targeted search for neutrinos in temporal and spatial coincidence with the gravitational wave events detected by the Advanced LIGO detectors, GW150914, GW151226 and GW170104, and on their implications for the total energy radiated in EeV neutrinos by identified sources of gravitational waves.

*XVII International Workshop on Neutrino Telescopes
13-17 March 2017
Venezia, Italy*

*Speaker.

1. Introduction

Observation of ultra-high energy (UHE) neutrinos in the 10^{18} eV (1 EeV) range can provide insight into the challenge of unveiling the origin and nature of the ultra-high energy cosmic rays (UHECR) [1, 2]. Despite the high level of precision in cosmic-ray measurements reached at current experiments such as the Pierre Auger Observatory [3], the results can be interpreted by different astrophysical scenarios without allowing one to conclude unambiguously about the origin of UHE-CRs. The key role of UHE neutrinos to solve this puzzle can be understood as follows. Neutrinos are expected from the interaction of UHECRs with matter and/or radiation at their sources [4] and with photons of the cosmic microwave background during propagation through the Universe [5]. Unlike cosmic rays, neutrinos point directly to their production sites, without being deflected in the galactic and extragalactic magnetic fields. Unlike photons, also expected from cosmic-ray interactions, neutrinos travel undisturbed from their sources carrying information about their production mechanisms. Therefore, the (non)-observation of UHE neutrinos may be the only probe of the dominant scenario of UHECR production.

Although the Pierre Auger Observatory was primarily conceived to measure UHECRs, it has shown an excellent sensitivity to EeV neutrino flux due to its vast collecting area and its ability to efficiently discriminate between neutrinos and hadronic cosmic rays. In this contribution we present an update to the search for UHE neutrinos with the Surface Detector (SD) of the Pierre Auger. It also includes the report on the recent targeted search for neutrinos above 100 PeV in coincidence with the gravitational wave (GW) events detected by the Advanced LIGO detectors, GW150914 [6, 7], GW151226 [8] and GW170104 [9]. These events were inferred to have been produced by binary Black Hole (BH) mergers, which might provide a potential environment where cosmic rays can be accelerated to the highest energies and produce neutrinos if there are magnetic fields and disk debris remaining from the formation of the two BHs [10, 11].

2. Searching for UHE neutrinos at the Pierre Auger Observatory

The principle for identification of neutrinos is founded on the fact that while cosmic rays (protons and nuclei), and even photons, interact shortly after entering the atmosphere, neutrinos can initiate showers quite deep. At large zenith angles, the electromagnetic (EM) component of extensive air showers (EAS) induced by cosmic rays gets absorbed in the large amount of atmosphere traversed and only the muon component reaches ground level. But if showers are induced deeply, a considerable amount of EM component reaches ground. Therefore as the zenith angle increases it becomes easier to discriminate the neutrino-induced EAS. Neutrino identification is then based on the selection of showers that arrive with large zenith angles with respect to the vertical (the so-called inclined showers) and rich on EM component.

The Surface Detector (SD) of the Pierre Auger Observatory consists of an array of 1600 water-Cherenkov detectors (WCD) deployed over an area of ~ 3000 km², arranged in a triangular grid of 1.5 km spacing, that samples at ground level the secondary particles of air showers initiated by primary cosmic rays in the atmosphere [3]. It was designed to measure the time structure of the signals produced by the passage of shower particles with 25 ns resolution and to be sensitive to showers arriving at extremely large zenith angles. Although the SD is not separately sensitive to the muonic

and EM components of the shower, nor to the depth at which the shower is initiated, the measurement of the time structure of the signal in the WCD allows one to distinguish narrow traces in time typical of shower fronts dominated by muons (as is the case in inclined showers initiated high in the atmosphere), from the broad signals in time a distinctive feature of shower fronts with a significant EM component as expected in inclined showers initiated close to the ground. These capabilities make the SD an efficient detector of UHE neutrinos with energies above 100 PeV. In particular, with the SD we can search for two types of neutrino-induced showers: (1) Earth-skimming (ES) showers initiated by tau neutrinos (ν_τ) that travel in a slightly upward direction, skim the Earth's crust and interact through charged current (CC) relatively close to the surface and induce a tau lepton that can escape the Earth and decay in flight in the atmosphere, close to the SD. Typically, only ν_τ -induced showers with zenith angles $90^\circ < \theta < 95^\circ$ may be identified [12]. (2) Showers initiated by neutrinos of any flavour moving down at zenith angles $\theta > 60^\circ$ that interact through both CC and neutral current (NC) with nuclei in the atmosphere and induce EAS near the ground [12, 13]. These are referred to as downward-going (DG) neutrinos. For optimization purposes the search in this channel is performed in two angular subranges: (a) "low" zenith angle (DGL) corresponding to $60^\circ < \theta < 75^\circ$ and (b) "high" zenith angle (DGH) with $75^\circ < \theta < 90^\circ$. Downward-going showers induced by ν_τ interacting in the mountains surrounding the Auger Observatory are also included in the DG channel.

The search methods for UHE neutrinos in the three channels described above (ES, DGH, DGL) were designed by exploiting the different characteristics of the showers in each angular window with the aid of Monte Carlo (MC) simulations. Although the particular searches for ES, DG, and DGH events require independent procedures for event selection, neutrino identification and exposure calculation, the general strategy is common: pre-selection of rather inclined events followed by a selection of neutrino candidates based on a single optimized variable. Inclined events are easily selected from the pattern of the triggered WCD stations at the ground that typically exhibit elongated patterns along the direction of arrival, well described by an ellipse with a high eccentricity. Another indication of inclined events is that the apparent speed of the trigger between station pairs in the event has an average value concentrated around the speed of light (c) and a small spread. In the DGL and DGH selections, the zenith angle θ_{rec} of the event is reconstructed and a cut on it is placed. To separate neutrinos candidates from the background of cosmic-ray showers, several observables related to the width of the signal trace are used depending on the specific selection. A Time-over-Threshold (ToT) trigger is usually present in WCDs with signals extending in time, while narrow signals induce other local triggers. Also the Area-over-Peak ratio (AoP), defined as the ratio of the integral of the digitized signal trace to its peak value, serves as a variable to discriminate broad from narrow shower fronts. For the ES selection the average AoP of the triggered stations, $\langle \text{AoP} \rangle$, is chosen as a discrimination variable for data after June 2010 while for earlier data the fraction of stations in the event with a ToT local trigger is used (see [14]). For the DGH (DGL) selection the individual AoP of the 4 (4 or 5) stations that trigger first (closest to shower core) in each event are combined in a linear Fisher-discriminant polynomial. In the DGL selection it is also required that at least 75% of the triggered stations closest to the core have a ToT local trigger.

The actual values of the neutrino selection cuts (above which events are classified as potential neutrino candidates) are decided *a priori* comparing the tails of the distributions of the $\langle \text{AoP} \rangle$ and

Fisher discriminant for simulated neutrino events to those taken from a small fraction of the data assumed to be overwhelmingly made up of background cosmic-ray showers. These distributions have an exponential tail which can be easily extrapolated to find the value of the cut corresponding to a background rate of less than 1 event per 50 yr on the full SD array. Roughly $\sim 95\%$, $\sim 85\%$, and $\sim 60\%$ of the inclined neutrino events are kept after the ES, DGH, DGL selections, respectively. See [14] for full details of the selections and specific values of the cuts. Note that the search approach followed by the Pierre Auger Collaboration is therefore a "blind" analysis strategy where the remaining fraction of data is not used until the selection procedure is established, and then it is "unblinded" to search for neutrino candidates.

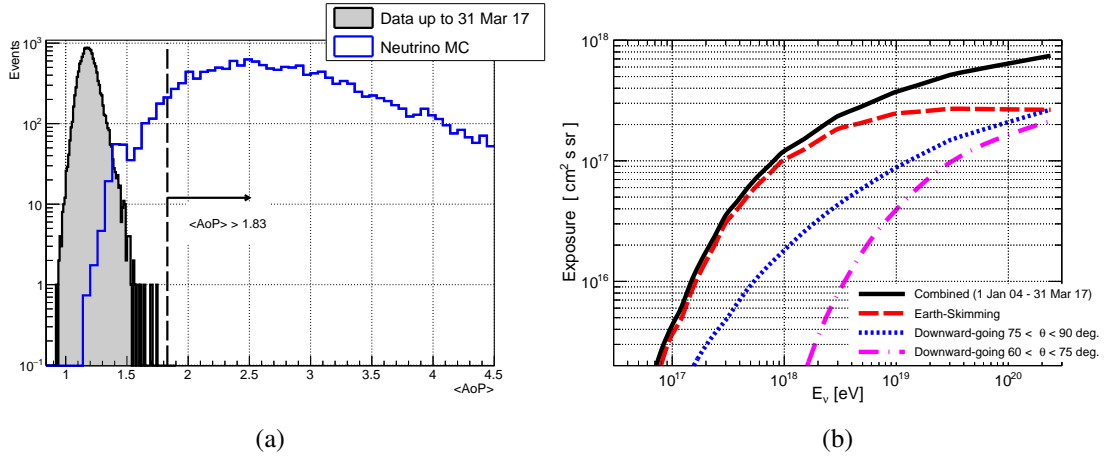


Figure 1: (a) Distributions of $\langle AoP \rangle$ (the variable used to identify neutrinos in the ES selection). The gray-filled histogram is the distribution for data after 1 June 2010 up to 31 March 2017 (training period excluded) and the blue-framed histogram are ES ν_τ events. The dashed vertical line represents the cut on $\langle AoP \rangle > 1.83$ above which a data event is classified as a neutrino candidate. (b) Total exposure (solid line) of the SD of the Pierre Auger Observatory (1 January 2004 - 31 March 2017) as a function of neutrino energy. Also shown are the individual exposures corresponding to ES (dashes), DGH (dots) and DGL (dot dashes) searches. For the DG channels the exposure represents the sum over the three neutrino flavours as well as CC and NC interactions. For the ES channels, only ν_τ CC interactions are relevant.

2.1 Data unblinding

The ES, DGH, DGL selection criteria in [14] were applied to data collected from 1 January 2004 to 31 March 2017 in a search for neutrino candidates. For each selection the corresponding training periods were excluded from the search. No neutrino candidates were found [15]. An example of the result of the unblinding is shown in Fig. 1 for the $\langle AoP \rangle$ variable in the ES analysis. Data events are far and to the left of the cut value at $\langle AoP \rangle > 1.83$. The same is true for the Fisher-discriminant distributions in the DGH and DGL selections.

In the absence of candidates in data collected in the search period, limits to diffuse and point-source fluxes of UHE neutrinos were placed as shown in the following sections.

2.2 SD exposure to UHE neutrinos

To obtain the neutrino bounds the exposure of the SD of the Pierre Auger Observatory to UHE neutrinos is needed. For its calculation the same criteria described above and in [14] are applied

to the neutrino simulated showers. The identification efficiency for each channel is obtained as the fraction of simulated events passing the cuts. For this purpose, a large set of MC simulations of neutrino-induced showers was performed, covering the whole relevant parameter space. For ES tau neutrinos, the efficiency depends on the energy of the emerging τ leptons, on the arrival direction and on the decay position of the τ above ground. For DG neutrinos, the identification efficiency depends on neutrino flavour, type of interaction (CC or NC), neutrino energy, arrival direction and distance measured from ground along the shower axis at which the neutrino is forced to interact in the simulations. For all the cases, the efficiencies also depend on time to account for the changing configuration of the SD array that was growing constantly during the construction phase (up to 2008), and continuous changes in the fraction of working stations. Although the number of working WCDs and their status are monitored every second, the approach adopted to calculate in an accurate and less time-consuming manner the actual identification efficiency is to sample them over real array configurations chosen every three days. Once the efficiencies are obtained, the calculation of the exposure involves folding them with the SD array aperture and with interaction/decay probabilities depending on the search channel. An integration over the whole parameter space except for the neutrino energy E_ν and in time over the search periods yields the exposure for each of the selections. The results of the exposure calculation for the ES, DGH and DGL selection channels are displayed in Fig. 1 along with the combined exposure assuming equal fluxes for all neutrino flavours at Earth. The ES channel dominates the exposure due to both the longer search period and the much larger neutrino conversion in the denser target of the Earth's crust compared to the atmosphere.

A study of the main sources of systematic uncertainties in the combined exposure has been performed [14]. The major contributions in terms of deviation from a reference exposure comes from the knowledge of neutrino-induced shower simulations ($\sim +4\%$, -3%), of the neutrino cross-section and τ energy loss ($\sim +34\%$, -28%) and the topography around the Observatory not accounted for in the exposure calculation in the ES channel ($\sim +15\%$, 0%).

3. Limits to the diffuse flux of UHE neutrinos

Using the combined exposure $\mathcal{E}(E_\nu)$ and assuming a differential flux $\Phi(E_\nu) = k E_\nu^{-2}$ as well as a $\nu_e : \nu_\mu : \nu_\tau = 1 : 1 : 1$ flavour ratio, an upper limit on the value of the normalization k can be obtained as $k = \frac{N_{\text{up}}}{\int_{E_\nu} E_\nu^{-2} \mathcal{E}(E_\nu) dE_\nu}$. In a semi-Bayesian extension of the Feldman-Cousins approach to include the systematic uncertainties in the exposure, if no events are observed the 90% C.L. limit is set for a flux predicting $N_{\text{up}} = 2.39$ events. The single-flavour 90% C.L. limit is $k_{90} < 5 \times 10^{-9} \text{GeV cm}^{-2} \text{s}^{-1} \text{sr}^{-1}$ [15] and applies in the energy interval from 0.1 to 25 EeV where $\sim 90\%$ of the total rate is expected. The relative contributions of the ES:DGH:DGL channels to the total expected event rate are $\sim 0.79 : 0.18 : 0.03$ respectively, and those of the electron:muon:tau neutrino flavours are $\sim 0.10 : 0.04 : 0.86$ respectively. The search period corresponds to an equivalent of nearly 10 years of a complete Auger SD array working continuously, which represents an increase of roughly 4 years of data with respect to previous results [14]. The limit is shown in Fig. 2, along with its representation in differential format calculated integrating the neutrino flux over consecutive energy bins of width 0.5 in $\log_{10} E_\nu$. The differential limit allows to show at which

energies the sensitivity of the SD of the Auger Observatory peaks. Limits from other neutrino experiments are also shown in Fig. 2 as well as several models of neutrino flux production.

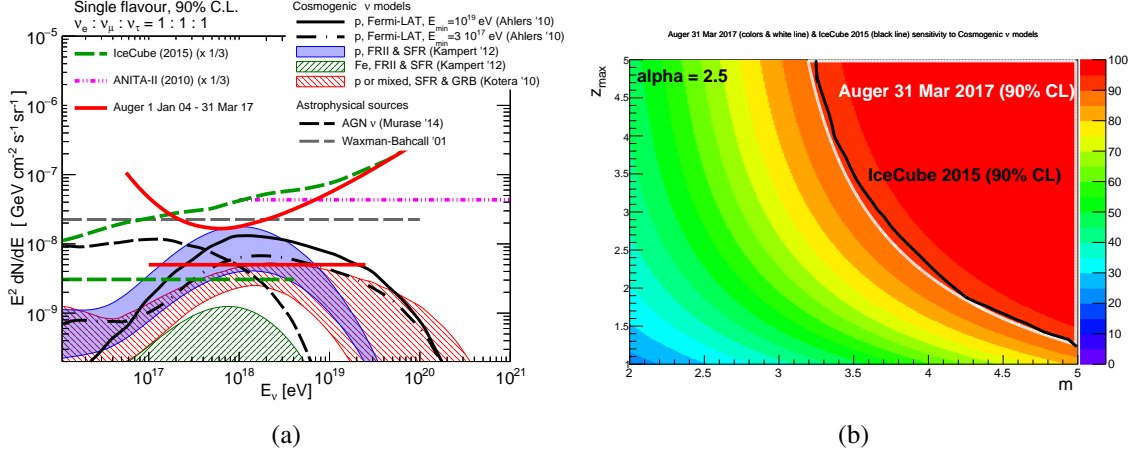


Figure 2: (a) Integral (straight red line) and differential upper limits to the normalization of the diffuse flux of UHE neutrinos (at 90% C.L.) from the Pierre Auger Observatory (curved red line). Also shown are the corresponding limits for ANITA-II [16] and IceCube [17] collaborations and the expected fluxes for several cosmogenic neutrino models [18, 19, 20] as well as astrophysical ν bound predictions [21, 22]. (b) Constrains on parameter space for cosmological neutrinos in proton models (assuming a power law $dN/dE \approx E^{-2.5}$ at the sources) as a function of m (source evolution) and z_{max} (maximum redshift of the sources) following [23]. Coloured areas represent different C.L. of exclusion. The region above the white (black) line is excluded at 90% C.L. by Auger (IceCube [17]) data.

By inspecting Fig. 2 it is clear that the SD of Auger Observatory is well suited for detecting cosmogenic neutrinos. Different models for cosmogenic ν 's that attempt to explain the origin of the cosmic rays are excluded at the 90% C.L., particularly those that assume a pure primary proton composition injected at the sources and strong (FRII-type) evolution of the sources with redshift [18]. Some models bounded by GeV γ -ray flux observations by Fermi-LAT [19] are also excluded. A model that assumes protons with moderate evolution close to that of SFR [20] is disfavoured. Using a conservative analytical approximation of the cosmogenic neutrino flux, exclusion plots can be made as functions of the most relevant parameters for cosmogenic ν models, namely: the source evolution (m), the maximum redshift to which the cosmic ray is integrated (z_{max}), the spectral index (α), and the maximum energy of the cosmic ray flux (E_{max}) [23]. The corresponding plot for $\alpha = 2.5$ and for $E_{\text{max}} = 300$ EeV is shown in Fig. 2. Also some models of neutrino production in astrophysical sources such as radio-loud Active Galactic Nuclei (AGN) [21] are excluded at more than 90% C.L.

4. Limits to point-like sources of UHE neutrinos

The neutrino search at the Pierre Auger Observatory is limited to highly inclined showers and thus, at each instant, neutrinos can be detected only from a specific portion of the sky corresponding to the zenith angle ranges of the selections. The sky coverage provided by the ES channel reaches declinations δ between -54.5° and 59.5° . Concerning the DG channels, they enhance the visible δ

band towards the south all the way to -84.5° covering a large fraction of the sky. The point-source exposure $\mathcal{E}(E_\nu, \delta)$ is obtained in a similar way as the diffuse exposure but avoiding the integration in solid angle and taking into account that the identification efficiency depends on the zenith angle θ , while the θ of the source depends on sidereal time.

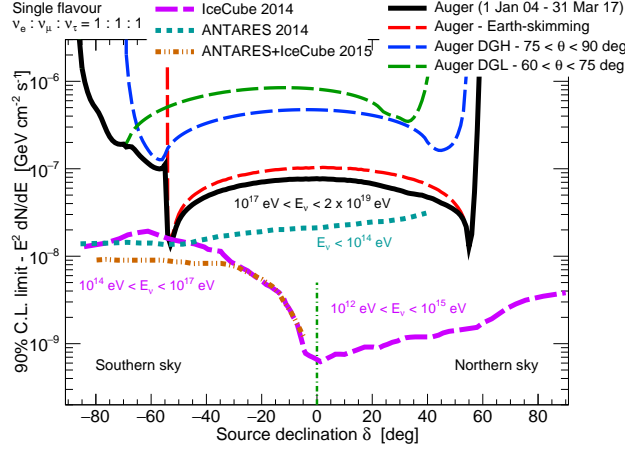


Figure 3: Upper limit (at 90% C.L.) to the normalization of a E_ν^{-2} differential neutrino flux from a point source as a function of the declination of the source, as obtained from the Pierre Auger Observatory (solid line). Individual limits for ES, DGH and DGL searches are also displayed as labeled. Also shown are the sensitivities for ANTARES [25], IceCube [26] and a combination of both [27].

The non-observation of neutrino candidates is cast into a bound on point-like sources which is calculated as a function of δ , assuming a point source flux which decreases in energy as $k^{\text{PS}} E_\nu^{-2}$ and a flavour ratio of 1:1:1. The combined and individual limits are shown in Fig. 3, for data that represents an increase of about 7 years of full exposure with respect to previous results [24], along with sensitivities for other neutrino experiments that cover different energy ranges.

5. Targeted search for neutrinos in coincidence with the Gravitational Wave events

The observation of GW events with the Advanced LIGO detectors compatible with having arisen from the merger of BHs in binary system has motivated a targeted search for neutrinos in temporal and spatial coincidence with them. The same identification criteria explained in Sec. 2 were applied to data collected with the Auger Observatory close in time and position with events GW150914, GW151226, GW170104 and the candidate event LVT151012. In each case the search was performed within two time windows: (1) ± 500 s around the UTC time of occurrence of the GW event, motivated by an upper limit to the duration of the prompt phase of Gamma Ray Bursts (GRBs) [28], when typically PeV neutrinos are thought to be produced in interactions of accelerated CRs and gamma rays within the GRB itself; (2) 1-day window after the GW event, driven by a conservative upper limit to the duration of the GRB afterglows, where UHE neutrinos are expected from the interactions of UHECRs with the lower-energy photons of the GRB afterglow (see [29] for a review). The spatial coincidence requirement is for neutrinos to come from a direction enclosed in the large at 90% C.L. contour (a broad region of few hundreds of square degrees) set by

the LIGO collaboration for the positions of the events. Because of the zenith angle restrictions of the search channels the visible part of the sky is limited at any instant.

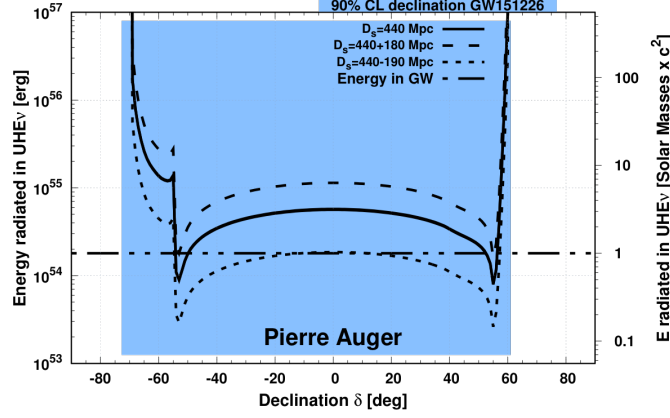


Figure 4: Constraints on the energy radiated in UHE neutrinos (per flavour) from the source of GW151226 as a function of the equatorial declination δ . Energies above the solid line, assuming the luminosity distance to the source $D_s = 440$ Mpc, are excluded at the 90% C.L. from the non-observation of UHE neutrinos in Auger. The dashed lines correspond to the 90% C.L. interval of possible distances to the source. For reference the dot-dashed horizontal line represents $E_{\text{GW}} \simeq 5.4 \times 10^{54}$ erg, the inferred energy radiated in gravitational waves from GW151226 [8]. The shaded region indicates the 90% C.L. declination band of this GW event.

In the short time-window there is a marginal overlap between the 90% C.L. position of GW150914 and the corresponding field of view of the SD for the DGH channel, while there is a substantial overlap between the sky coverage with ES and DG channels and the reported positions for GW151226, GW170104 and LVT151012. No neutrino candidates were found in coincidence with any of the GW events (and the candidate one), in fact, no inclined background showers from cosmic rays were observed neither [30, 15].

In the 1-day period after the GW the instantaneous exposure is averaged over a sidereal day. The overlap with the field of view of the SD is large for GW150914, GW170104 and LVT151012 and practically all the 90% C.L. declination band for GW151226. Although inclined showers were observed within the 1-day periods after the GW events none of them fulfilled the neutrino identification criteria [30, 15].

The absence of neutrino candidates allows one to place upper limits to the flux of UHE neutrinos from the GW events as a function of equatorial declination δ , assuming a standard E_ν^{-2} spectrum. In addition, a bound on the total energy radiated from the GW source in UHE neutrinos can be obtained using the luminosity distances quoted for the events. Results depend on the direction and distance of the source. As an example the limit for the event GW151226 is shown in Fig. 4. The constraints on total energy can be expressed as fractions f_ν of energy in UHE neutrinos relative to the energy radiated in gravitational waves. For example for the event shown in Fig. 4 the best upper limit on this fraction is $f_\nu(\delta = 55^\circ) < 44.1\%$. See [30] for further details on the analysis.

6. Conclusion

The Pierre Auger Observatory has been demonstrated to be an effective detector for neutrinos of all flavours with energies around 100 PeV and above, covering sky directions with equatorial declinations from $\sim -80^\circ$ to $+60^\circ$. Given the non-observation of neutrino candidates in data collected with the SD from 1 January 2004 to 31 March 2017 improved strong limits to diffuse fluxes of UHE neutrinos have been obtained, allowing one to constrain the parameter space of cosmogenic neutrinos and to prove some models of neutrino production in astrophysical sources. The Pierre Auger Observatory is indeed the first air shower array to set a limit below the Waxman-Bahcall flux. Also new limits on steady point sources have also been obtained.

Finally a targeted search for UHE neutrinos in time and spatial coincidence with the LIGO GW events from BH mergers has yielded limits on a possible UHE neutrino emission from the GW sources and on its energy budget. In this new era for multi-messenger astronomy, more GW events are expected in the near future and the neutrino follow-up search with the SD of the Auger Observatory will provide an additional tool to identify the GW sources and contribute to constrain the properties of such astrophysical phenomena, complementary to the TeV-PeV region covered by IceCube and ANTARES.

References

- [1] D. Seckel and T. Stanev, Phys. Rev. Lett. **95** (2005) 141101.
- [2] D. Allard *et al.*, JCAP **0609** (2006) 005.
- [3] A. Aab *et al.* [Pierre Auger Collaboration], Nucl. Instrum. Meth. A **798** (2015) 172.
- [4] J. K. Becker, Phys. Rept. **458** (2008) 173.
- [5] V. S. Berezinsky and G. T. Zatsepin, Phys. Lett. **28B** (1969) 423.
- [6] B. P. Abbott *et al.* [LIGO Scientific and Virgo Collab.], Phys. Rev. Lett. **116** (2016) no.6, 061102.
- [7] B. P. Abbott *et al.* [LIGO Scientific and Virgo Collab.], Phys. Rev. Lett. **116** (2016) no.24, 241102.
- [8] B. P. Abbott *et al.* [LIGO Scientific and Virgo Collab.], Phys. Rev. Lett. **116** (2016) no.24, 241103.
- [9] B. P. Abbott *et al.* [LIGO Scientific and VIRGO Collab.], Phys. Rev. Lett. **118** (2017) no.22, 221101.
- [10] K. Murase *et al.*, Astrophys. J. **822** (2016) no.1, L9.
- [11] K. Kotera and J. Silk, Astrophys. J. **823** (2016) no.2, L29.
- [12] K. S. Capelle *et al.*, Astropart. Phys. **8** (1998) 321; X. Bertou *et al.*, Astropart. Phys. **17** (2002) 183; D. Fargion, Astrophys. J. **570** (2002) 909.
- [13] I. Valiño, Ph.D. thesis, Universidad de Santiago de Compostela, ISBN: 9788497509664 (2008).
- [14] A. Aab *et al.* [Pierre Auger Collaboration], Phys. Rev. D **91** (2015), 092008.
- [15] E. Zas for the Pierre Auger Collaboration, PoS (2017) 972, arXiv:1708.06592.
- [16] P. W. Gorham *et al.* [ANITA Collaboration], Phys. Rev. D **85** (2012) 049901.
- [17] M. G. Aartsen *et al.* [IceCube Collaboration], Phys. Rev. Lett. **117** (2016) no.24, 241101.
- [18] K. H. Kampert and M. Unger, Astropart. Phys. **35** (2012) 660.

- [19] M. Ahlers *et al.*, *Astropart. Phys.* **34** (2010) 106.
- [20] K. Kotera, D. Allard and A. V. Olinto, *JCAP* **1010** (2010) 013.
- [21] K. Murase, Y. Inoue and C. D. Dermer, *Phys. Rev. D* **90** (2014) no.2, 023007.
- [22] E. Waxman and J. N. Bahcall, *Phys. Rev. D* **64** (2001) 023002.
- [23] S. Yoshida and A. Ishihara, *Phys. Rev. D* **85** (2012) 063002.
- [24] P. Abreu *et al.* [Pierre Auger Collaboration], *Astrophys. J.* **755** (2012) L4.
- [25] S. Adrian-Martinez *et al.* [ANTARES Collaboration], *Astrophys. J.* **786** (2014) L5.
- [26] M. G. Aartsen *et al.* [IceCube Collaboration], *Astrophys. J.* **796** (2014) no.2, 109.
- [27] S. Adrian-Martinez *et al.* [ANTARES and IceCube Collab.], *Astrophys. J.* **823** (2016) no.1, 65.
- [28] B. Baret *et al.*, *Astropart. Phys.* **35** (2011) 1.
- [29] P. Meszaros, *Rept. Prog. Phys.* **69** (2006) 2259.
- [30] A. Aab *et al.* [Pierre Auger Collaboration], *Phys. Rev. D* **94** (2016) no.12, 122007.

The Pierre Auger Collaboration

A. Aab⁶⁴, P. Abreu⁷¹, M. Aglietta^{49,48}, I. Al Samarai³⁰, I.F.M. Albuquerque¹⁷, I. Allekotte¹, A. Almela^{8,11}, J. Alvarez Castillo⁶³, J. Alvarez-Muñiz⁷⁹, G.A. Anastasi³⁹, L. Anchordoqui⁸², B. Andrada⁸, S. Andringa⁷¹, C. Aramo⁴⁶, F. Arqueros⁷⁷, N. Arsene⁷³, H. Asorey^{1,25}, P. Assis⁷¹, J. Aublin³⁰, G. Avila^{9,10}, A.M. Badescu⁷⁴, A. Balaceanu⁷², F. Barbato⁵⁵, R.J. Barreira Luz⁷¹, J.J. Beatty⁸⁷, K.H. Becker³², J.A. Bellido¹², C. Berat³¹, M.E. Bertaina^{57,48}, X. Bertou¹, P.L. Biermann^b, P. Billoir³⁰, J. Biteau²⁹, S.G. Blaess¹², A. Blanco⁷¹, J. Blazek²⁷, C. Bleve^{51,44}, M. Boháčová²⁷, D. Boncioli^{41,d}, C. Bonifazi²³, N. Borodai⁶⁸, A.M. Botti^{8,34}, J. Brack^h, I. Brancus⁷², T. Bretz³⁶, A. Bridgeman³⁴, F.L. Briechele³⁶, P. Buchholz³⁸, A. Bueno⁷⁸, S. Buitink⁶⁴, M. Buscemi^{53,43}, K.S. Caballero-Mora⁶¹, L. Caccianiga⁵⁴, A. Cancio^{11,8}, F. Canfora⁶⁴, L. Caramete⁷³, R. Caruso^{53,43}, A. Castellina^{49,48}, G. Cataldi⁴⁴, L. Cazon⁷¹, A.G. Chavez⁶², J.A. Chinellato¹⁸, J. Chudoba²⁷, R.W. Clay¹², A. Cobos⁸, R. Colalillo^{55,46}, A. Coleman⁸⁸, L. Collica⁴⁸, M.R. Coluccia^{51,44}, R. Conceição⁷¹, G. Consolati⁵⁴, F. Contreras^{9,10}, M.J. Cooper¹², S. Coutu⁸⁸, C.E. Covault⁸⁰, J. Cronin⁸⁹, S. D'Amico^{50,44}, B. Daniel¹⁸, S. Dasso^{5,3}, K. Daumiller³⁴, B.R. Dawson¹², R.M. de Almeida²⁴, S.J. de Jong^{64,66}, G. De Mauro⁶⁴, J.R.T. de Mello Neto²³, I. De Mitri^{51,44}, J. de Oliveira²⁴, V. de Souza¹⁶, J. Debatin³⁴, O. Deligny²⁹, C. Di Giulio^{56,47}, A. Di Matteo^{52,42}, M.L. Díaz Castro¹⁸, F. Diogo⁷¹, C. Dobrigkeit¹⁸, J.C. D'Olivo⁶³, Q. Dorosti³⁸, R.C. dos Anjos²², M.T. Dova⁴, A. Dundovic³⁷, J. Ebr²⁷, R. Engel³⁴, M. Erdmann³⁶, M. Erfani³⁸, C.O. Escobar^f, J. Espadanal⁷¹, A. Etchegoyen^{8,11}, H. Falcke^{64,67,66}, G. Farrar⁸⁵, A.C. Fauth¹⁸, N. Fazzini^f, F. Fenu⁵⁷, B. Fick⁸⁴, J.M. Figueira⁸, A. Filipčič^{75,76}, O. Fratu⁷⁴, M.M. Freire⁶, T. Fujii⁸⁹, A. Fuster^{8,11}, R. Gaior³⁰, B. García⁷, D. Garcia-Pinto⁷⁷, F. Gaté^e, H. Gemmeke³⁵, A. Gherghel-Lascu⁷², P.L. Ghia²⁹, U. Giaccari²³, M. Giammarchi⁴⁵, M. Giller⁶⁹, D. Glas⁷⁰, C. Glaser³⁶, G. Golup¹, M. Gómez Berisso¹, P.F. Gómez Vitale^{9,10}, N. González^{8,34}, A. Gorgi^{49,48}, P. Gorhamⁱ, A.F. Grillo⁴¹, T.D. Grubb¹², F. Guarino^{55,46}, G.P. Guedes¹⁹, M.R. Hampel⁸, P. Hansen⁴, D. Harari¹, T.A. Harrison¹², J.L. Harton^h, A. Haungs³⁴, T. Hebbeker³⁶, D. Heck³⁴, P. Heimann³⁸, A.E. Herve³³, G.C. Hill¹², C. Hojvat^f, E. Holt^{34,8}, P. Homola⁶⁸, J.R. Hörandel^{64,66}, P. Horvath²⁸, M. Hrabovský²⁸, T. Huege³⁴, J. Hulsman^{8,34}, A. Insolia^{53,43}, P.G. Isar⁷³, I. Jandt³², S. Jansen^{64,66}, J.A. Johnsen⁸¹, M. Josebachuili⁸, J. Jurysek²⁷, A. Kääpä³², O. Kambeitz³³, K.H. Kampert³², I. Katkov³³, B. Keilhauer³⁴, N. Kemmerich¹⁷, E. Kemp¹⁸, J. Kemp³⁶, R.M. Kieckhafer⁸⁴, H.O. Klages³⁴, M. Kleifges³⁵, J. Kleinfeller⁹, R. Krause³⁶, N. Krohm³², D. Kuempel³⁶, G. Kukec Mezek⁷⁶, N. Kunka³⁵, A. Kuotb Awad³⁴, D. LaHurd⁸⁰, M. Lauscher³⁶, R. Legumina⁶⁹, M.A. Leigui de Oliveira²¹, A. Letessier-Selvon³⁰, I. Lhenry-Yvon²⁹, K. Link³³, D. Lo Presti⁵³, L. Lopes⁷¹, R. López⁵⁸, A. López Casado⁷⁹, Q. Luce²⁹, A. Lucero^{8,11}, M. Malacari⁸⁹, M. Mallamaci^{54,45}, D. Mandat²⁷, P. Mantsch^f, A.G. Mariazzi⁴, I.C. Mariş¹³, G. Marsella^{51,44}, D. Martello^{51,44}, H. Martinez⁵⁹, O. Martínez Bravo⁵⁸, J.J. Masías Meza³, H.J. Mathes³⁴, S. Mathys³², J. Matthews⁸³, J.A.J. Matthews^j, G. Matthiae^{56,47}, E. Mayotte³², P.O. Mazur^f, C. Medina⁸¹, G. Medina-Tanco⁶³, D. Melo⁸, A. Menshikov³⁵, K.-D. Merenda⁸¹, S. Michal²⁸, M.I. Micheletti⁶, L. Middendorf³⁶, L. Miramonti^{54,45}, B. Mitrica⁷², D. Mockler³³, S. Mollerach¹, F. Montanet³¹, C. Morello^{49,48}, M. Mostafa⁸⁸, A.L. Müller^{8,34}, G. Müller³⁶, M.A. Muller^{18,20}, S. Müller^{34,8}, R. Mussa⁴⁸, I. Naranjo¹, L. Nellen⁶³, P.H. Nguyen¹², M. Niculescu-Oglinzanu⁷², M. Niechciol³⁸, L. Niemietz³², T. Niggemann³⁶, D. Nitz⁸⁴, D. Nosek²⁶, V. Novotny²⁶, L. Nožka²⁸, L.A. Núñez²⁵, L. Ochilo³⁸, F. Oikonomou⁸⁸, A. Olinto⁸⁹, M. Palatka²⁷, J. Pallotta², P. Papenbreer³², G. Parente⁷⁹, A. Parra⁵⁸, T. Paul^{86,82}, M. Pech²⁷, F. Pedreira⁷⁹, J. Pękala⁶⁸, R. Pelayo⁶⁰, J. Peña-Rodríguez²⁵, L. A. S. Pereira¹⁸, M. Perlín⁸, L. Perrone^{51,44}, C. Peters³⁶, S. Petrera^{52,39,42}, J. Phuntsok⁸⁸, R. Piegaia³, T. Pierog³⁴, P. Pieroni³, M. Pimenta⁷¹, V. Pirronello^{53,43}, M. Platino⁸, M. Plum³⁶, C. Porowski⁶⁸, R.R. Prado¹⁶, P. Privitera⁸⁹, M. Prouza²⁷, E.J. Quel², S. Querschfeld³², S. Quinn⁸⁰, R. Ramos-Pollán²⁵, J. Rautenberg³², D. Ravignani⁸, B. Revenu^e, J. Ridky²⁷, M. Risse³⁸, P. Ristori², V. Rizi^{52,42}, W. Rodrigues de Carvalho¹⁷, G. Rodriguez Fernandez^{56,47}, J. Rodriguez Rojo⁹,

D. Rogozin³⁴, M.J. Roncoroni⁸, M. Roth³⁴, E. Roulet¹, A.C. Rovero⁵, P. Ruehl³⁸, S.J. Saffi¹², A. Saftoiu⁷², F. Salamida^{52,42}, H. Salazar⁵⁸, A. Saleh⁷⁶, F. Salesa Greus⁸⁸, G. Salina⁴⁷, F. Sánchez⁸, P. Sanchez-Lucas⁷⁸, E.M. Santos¹⁷, E. Santos⁸, F. Sarazin⁸¹, R. Sarmento⁷¹, C.A. Sarmiento⁸, R. Sato⁹, M. Schauer³², V. Scherini⁴⁴, H. Schieler³⁴, M. Schimp³², D. Schmidt^{34,8}, O. Scholten^{65,c}, P. Schovánek²⁷, F.G. Schröder³⁴, A. Schulz³³, J. Schumacher³⁶, S.J. Sciutto⁴, A. Segreto^{40,43}, M. Settimo³⁰, A. Shadkam⁸³, R.C. Shellard¹⁴, G. Sigl³⁷, G. Silli^{8,34}, O. Sima⁸, A. Śmiałkowski⁶⁹, R. Šmída³⁴, G.R. Snow⁹⁰, P. Sommers⁸⁸, S. Sonntag³⁸, J. Sorokin¹², R. Squartini⁹, D. Stanca⁷², S. Stanič⁷⁶, J. Stasielak⁶⁸, P. Stassi³¹, F. Strafella^{51,44}, F. Suarez^{8,11}, M. Suarez Durán²⁵, T. Sudholz¹², T. Suomijärvi²⁹, A.D. Supanitsky⁵, J. Šupík²⁸, J. Swain⁸⁶, Z. Szadkowski⁷⁰, A. Taboada³³, O.A. Taborda¹, A. Tapia⁸, V.M. Theodoro¹⁸, C. Timmermans^{66,64}, C.J. Toderó Peixoto¹⁵, L. Tomankova³⁴, B. Tomé⁷¹, G. Torralba Elípe⁷⁹, P. Travnicek²⁷, M. Trini⁷⁶, R. Ulrich³⁴, M. Unger³⁴, M. Urban³⁶, J.F. Valdés Galicia⁶³, I. Valiño⁷⁹, L. Valore^{55,46}, G. van Aar⁶⁴, P. van Bodegom¹², A.M. van den Berg⁶⁵, A. van Vliet⁶⁴, E. Varela⁵⁸, B. Vargas Cárdenas⁶³, G. Varnerⁱ, R.A. Vázquez⁷⁹, D. Veberič³⁴, C. Ventura²³, I.D. Vergara Quispe⁴, V. Verzi⁴⁷, J. Vicha²⁷, L. Villaseñor⁶², S. Vorobiov⁷⁶, H. Wahlberg⁴, O. Wainberg^{8,11}, D. Walz³⁶, A.A. Watson^a, M. Weber³⁵, A. Weindl³⁴, L. Wiencke⁸¹, H. Wilczyński⁶⁸, M. Wirtz³⁶, D. Wittkowski³², B. Wundheiler⁸, L. Yang⁷⁶, A. Yushkov⁸, E. Zas⁷⁹, D. Zavrtanik^{76,75}, M. Zavrtanik^{75,76}, A. Zepeda⁵⁹, B. Zimmermann³⁵, M. Ziolkowski³⁸, Z. Zong²⁹, F. Zuccarello^{53,43}

— • —

¹ Centro Atómico Bariloche and Instituto Balseiro (CNEA-UNCuyo-CONICET), Argentina

² Centro de Investigaciones en Láseres y Aplicaciones, CITEDEF and CONICET, Argentina

³ Departamento de Física and Departamento de Ciencias de la Atmósfera y los Océanos, FCEyN, Universidad de Buenos Aires, Argentina

⁴ IFLP, Universidad Nacional de La Plata and CONICET, Argentina

⁵ Instituto de Astronomía y Física del Espacio (IAFE, CONICET-UBA), Argentina

⁶ Instituto de Física de Rosario (IFIR) - CONICET/U.N.R. and Facultad de Ciencias Bioquímicas y Farmacéuticas U.N.R., Argentina

⁷ Instituto de Tecnologías en Detección y Astropartículas (CNEA, CONICET, UNSAM) and Universidad Tecnológica Nacional - Facultad Regional Mendoza (CONICET/CNEA), Argentina

⁸ Instituto de Tecnologías en Detección y Astropartículas (CNEA, CONICET, UNSAM), Centro Atómico Constituyentes, Comisión Nacional de Energía Atómica, Argentina

⁹ Observatorio Pierre Auger, Argentina

¹⁰ Observatorio Pierre Auger and Comisión Nacional de Energía Atómica, Argentina

¹¹ Universidad Tecnológica Nacional - Facultad Regional Buenos Aires, Argentina

¹² University of Adelaide, Australia

¹³ Université Libre de Bruxelles (ULB), Belgium

¹⁴ Centro Brasileiro de Pesquisas Físicas (CBPF), Brazil

¹⁵ Universidade de São Paulo, Escola de Engenharia de Lorena, Brazil

¹⁶ Universidade de São Paulo, Inst. de Física de São Carlos, São Carlos, Brazil

¹⁷ Universidade de São Paulo, Inst. de Física, São Paulo, Brazil

¹⁸ Universidade Estadual de Campinas (UNICAMP), Brazil

¹⁹ Universidade Estadual de Feira de Santana (UEFS), Brazil

²⁰ Universidade Federal de Pelotas, Brazil

²¹ Universidade Federal do ABC (UFABC), Brazil

²² Universidade Federal do Paraná, Setor Palotina, Brazil

²³ Universidade Federal do Rio de Janeiro (UFRJ), Instituto de Física, Brazil

²⁴ Universidade Federal Fluminense, Brazil

²⁵ Universidad Industrial de Santander, Colombia

- ²⁶ Charles University, Institute of Particle & Nuclear Physics, Faculty of Mathematics and Physics, Czech Republic
- ²⁷ Institute of Physics of the Czech Academy of Sciences, Czech Republic, Czech Republic
- ²⁸ Palacky University, RCPTM, Olomouc, Czech Republic
- ²⁹ Institut de Physique Nucléaire d'Orsay (IPNO), Université Paris-Sud, Univ. Paris/Saclay, CNRS-IN2P3, France, France
- ³⁰ Laboratoire de Physique Nucléaire et de Hautes Energies (LPNHE), Universités Paris 6 et Paris 7, CNRS-IN2P3, France
- ³¹ Laboratoire de Physique Subatomique et de Cosmologie (LPSC), Université Grenoble-Alpes, CNRS-IN2P3, France
- ³² Bergische Universität Wuppertal, Department of Physics, Germany
- ³³ Karlsruhe Institute of Technology, Institut für Experimentelle Kernphysik (IEKP), Germany
- ³⁴ Karlsruhe Institute of Technology, Institut für Kernphysik (IKP), Germany
- ³⁵ Karlsruhe Institute of Technology, Institut für Prozessdatenverarbeitung und Elektronik (IPE), Germany
- ³⁶ RWTH Aachen University, III. Physikalisches Institut A, Germany
- ³⁷ Universität Hamburg, II. Institut für Theoretische Physik, Germany
- ³⁸ Universität Siegen, Fachbereich 7 Physik - Experimentelle Teilchenphysik, Germany
- ³⁹ Gran Sasso Science Institute (INFN), L'Aquila, Italy
- ⁴⁰ INAF - Istituto di Astrofisica Spaziale e Fisica Cosmica di Palermo, Italy
- ⁴¹ INFN Laboratori Nazionali del Gran Sasso, Italy
- ⁴² INFN, Gruppo Collegato dell'Aquila, Italy
- ⁴³ INFN, Sezione di Catania, Italy
- ⁴⁴ INFN, Sezione di Lecce, Italy
- ⁴⁵ INFN, Sezione di Milano, Italy
- ⁴⁶ INFN, Sezione di Napoli, Italy
- ⁴⁷ INFN, Sezione di Roma "Tor Vergata", Italy
- ⁴⁸ INFN, Sezione di Torino, Italy
- ⁴⁹ Osservatorio Astrofisico di Torino (INAF), Torino, Italy
- ⁵⁰ Università del Salento, Dipartimento di Ingegneria, Italy
- ⁵¹ Università del Salento, Dipartimento di Matematica e Fisica "E. De Giorgi", Italy
- ⁵² Università dell'Aquila, Dipartimento di Scienze Fisiche e Chimiche, Italy
- ⁵³ Università di Catania, Dipartimento di Fisica e Astronomia, Italy
- ⁵⁴ Università di Milano, Dipartimento di Fisica, Italy
- ⁵⁵ Università di Napoli "Federico II", Dipartimento di Fisica "Ettore Pancini", Italy
- ⁵⁶ Università di Roma "Tor Vergata", Dipartimento di Fisica, Italy
- ⁵⁷ Università Torino, Dipartimento di Fisica, Italy
- ⁵⁸ Benemérita Universidad Autónoma de Puebla (BUAP), México
- ⁵⁹ Centro de Investigación y de Estudios Avanzados del IPN (CINVESTAV), México
- ⁶⁰ Unidad Profesional Interdisciplinaria en Ingeniería y Tecnologías Avanzadas del Instituto Politécnico Nacional (UPIITA-IPN), México
- ⁶¹ Universidad Autónoma de Chiapas, México
- ⁶² Universidad Michoacana de San Nicolás de Hidalgo, México
- ⁶³ Universidad Nacional Autónoma de México, México
- ⁶⁴ Institute for Mathematics, Astrophysics and Particle Physics (IMAPP), Radboud Universiteit, Nijmegen, Netherlands
- ⁶⁵ KVI - Center for Advanced Radiation Technology, University of Groningen, Netherlands
- ⁶⁶ Nationaal Instituut voor Kernfysica en Hoge Energie Fysica (NIKHEF), Netherlands
- ⁶⁷ Stichting Astronomisch Onderzoek in Nederland (ASTRON), Dwingeloo, Netherlands

- ⁶⁸ Institute of Nuclear Physics PAN, Krakow, Poland
- ⁶⁹ University of Łódź, Faculty of Astrophysics, Poland
- ⁷⁰ University of Łódź, Faculty of High-Energy Astrophysics, Poland
- ⁷¹ Laboratório de Instrumentação e Física Experimental de Partículas - LIP and Instituto Superior Técnico - IST, Universidade de Lisboa - UL, Portugal
- ⁷² “Horia Hulubei” National Institute for Physics and Nuclear Engineering, Romania
- ⁷³ Institute of Space Science, Bucharest-Magurele, Romania
- ⁷⁴ University Politehnica of Bucharest, Romania
- ⁷⁵ Experimental Particle Physics Department, J. Stefan Institute, Ljubljana, Slovenia
- ⁷⁶ Laboratory for Astroparticle Physics, University of Nova Gorica, Slovenia
- ⁷⁷ Universidad Complutense de Madrid, Spain
- ⁷⁸ Universidad de Granada and C.A.F.P.E., Spain
- ⁷⁹ Universidad de Santiago de Compostela, Spain
- ⁸⁰ Case Western Reserve University, Cleveland, OH, USA
- ⁸¹ Colorado School of Mines, Golden, CO, USA
- ⁸² Department of Physics and Astronomy, Lehman College, City University of New York, Bronx, NY, USA
- ⁸³ Louisiana State University, Baton Rouge, LA, USA
- ⁸⁴ Michigan Technological University, Houghton, MI, USA
- ⁸⁵ New York University, New York, NY, USA
- ⁸⁶ Northeastern University, Boston, MA, USA
- ⁸⁷ Ohio State University, Columbus, OH, USA
- ⁸⁸ Pennsylvania State University, University Park, PA, USA
- ⁸⁹ University of Chicago, Enrico Fermi Institute, Chicago, IL, USA
- ⁹⁰ University of Nebraska, Lincoln, NE, USA

^a School of Physics and Astronomy, University of Leeds, Leeds, United Kingdom

^b Max-Planck-Institut für Radioastronomie, Bonn, Germany

^c also at Vrije Universiteit Brussels, Brussels, Belgium

^d now at Deutsches Elektronen-Synchrotron (DESY), Zeuthen, Germany

^e SUBATECH, École des Mines de Nantes, CNRS-IN2P3, Université de Nantes

^f Fermi National Accelerator Laboratory, USA

^g University of Bucharest, Physics Department, Bucharest

^h Colorado State University, Fort Collins, CO

ⁱ University of Hawaii, Honolulu, HI

^j University of New Mexico, Albuquerque, NM

Acknowledgments

The successful installation, commissioning, and operation of the Pierre Auger Observatory would not have been possible without the strong commitment and effort from the technical and administrative staff in Malargüe. We are very grateful to the following agencies and organizations for financial support:

Argentina -- Comisión Nacional de Energía Atómica; Agencia Nacional de Promoción Científica y Tecnológica (ANPCyT); Consejo Nacional de Investigaciones Científicas y Técnicas (CONICET); Gobierno de la Provincia de Mendoza; Municipalidad de Malargüe; NDM Holdings and Valle Las Leñas; in gratitude for their continuing cooperation over land access; Australia -- the Australian Research Council; Brazil -- Conselho Nacional de Desenvolvimento Científico e Tecnológico (CNPq); Financiadora de Estudos e Projetos (FINEP); Fundação de Amparo à Pesquisa do Estado de Rio de Janeiro (FAPERJ); São Paulo Research Foundation (FAPESP) Grants No.\ 2010/07359-6 and No.\ 1999/05404-3; Ministério de Ciência e Tecnologia (MCT); Czech Republic -- Grant No.\ MSM T CR LG15014, LO1305, LM2015038 and

CZ.02.1.01/0.0/0.0/16_013/0001402; France -- Centre de Calcul IN2P3/CNRS; Centre National de la Recherche Scientifique (CNRS); Conseil Régional Ile-de-France; Département Physique Nucléaire et Corpusculaire (PNC-IN2P3/CNRS); Département Sciences de l'Univers (SDU-INSU/CNRS); Institut Lagrange de Paris (ILP) Grant No.\ LABEX ANR-10-LABX-63 within the Investissements d'Avenir Programme Grant No.\ ANR-11-IDEX-0004-02; Germany -- Bundesministerium für Bildung und Forschung (BMBF); Deutsche Forschungsgemeinschaft (DFG); Finanzministerium Baden-Württemberg; Helmholtz Alliance for Astroparticle Physics (HAP); Helmholtz-Gemeinschaft Deutscher Forschungszentren (HGF); Ministerium für Innovation, Wissenschaft und Forschung des Landes Nordrhein-Westfalen; Ministerium für Wissenschaft, Forschung und Kunst des Landes Baden-Württemberg; Italy -- Istituto Nazionale di Fisica Nucleare (INFN); Istituto Nazionale di Astrofisica (INAF); Ministero dell'Istruzione, dell'Università e della Ricerca (MIUR); CETEMPS Center of Excellence; Ministero degli Affari Esteri (MAE); Mexico -- Consejo Nacional de Ciencia y Tecnología (CONACYT) No.\ 167733; Universidad Nacional Autónoma de México (UNAM); PAPIIT DGAPA-UNAM; The Netherlands -- Ministerie van Onderwijs, Cultuur en Wetenschap; Nederlandse Organisatie voor Wetenschappelijk Onderzoek (NWO); Stichting voor Fundamenteel Onderzoek der Materie (FOM); Poland -- National Centre for Research and Development, Grants No.\ ERA-NET-ASPERA/01/11 and No.\ ERA-NET-ASPERA/02/11; National Science Centre, Grants No.\ 2013/08/M/ST9/00322, No.\ 2013/08/M/ST9/00728 and No.\ HARMONIA 5 -- 2013/10/M/ST9/00062; Portugal -- Portuguese national funds and FEDER funds within Programa Operacional Factores de Competitividade through Fundação para a Ciência e a Tecnologia (COMPETE); Romania -- Romanian Authority for Scientific Research ANCS; CNDI-UEFISCDI partnership projects Grants No.\ 20/2012 and No.194/2012 and PN 16 42 01 02; Slovenia -- Slovenian Research Agency; Spain -- Comunidad de Madrid; Fondo Europeo de Desarrollo Regional (FEDER) funds; Ministerio de Economía y Competitividad; Xunta de Galicia; European Community 7th Framework Program Grant No.\ FP7-PEOPLE-2012-IEF-328826; USA -- Department of Energy, Contracts No.\ DE-AC02-07CH11359, No.\ DE-FR02-04ER41300, No.\ DE-FG02-99ER41107 and No.\ DE-SC0011689; National Science Foundation, Grant No.\ 0450696; The Grainger Foundation; Marie Curie-IRSES/EPLANET; European Particle Physics Latin American Network; European Union 7th Framework Program, Grant No.\ PIRSES-2009-GA-246806; European Union's Horizon 2020 research and innovation programme (Grant No.\ 646623); and UNESCO.